EXAMINING VARIABILITY IN THE MECHANICAL PROPERTIES OF PARTS MANUFACTURED VIA POLYJET DIRECT 3D PRINTING

Michael W. Barclift and Christopher B. Williams
Design, Research, and Education for Additive Manufacturing Systems Laboratory
Department of Mechanical Engineering, Virginia Tech
REVIEWED, Accepted August 15, 2012

ABSTRACT

In Objet's PolyJet process, part layers are created by selectively inkjetting photopolymers onto a build substrate and then cured with ultraviolet lamps. With an eye towards using PolyJet as a manufacturing process to fabricate end-use products, the authors examine the sensitivity of part material properties to variation in process parameters. Specifically, a design of experiments is conducted using a full-factorial design to analyze the effects of three parameters on the specimens' tensile strength and tensile modulus: the in-build plane part orientation (X-Y), the out-of-build plane part orientation (Z), and the distance between specimens. Results show that part spacing has the largest effect on the tensile strength, but the three parameters produced no statistically significant effects on the tensile modulus. Orienting specimens in XZ orientation with minimal part spacing resulted in the highest tensile strength and modulus. Whereas, orienting specimens in the YZ orientation at the farthest part spacing led to the lowest mechanical properties.

Keywords: Objet, PolyJet, Design of Experiments, 3D Printing

1. INTRODUCTION

PolyJet Direct 3D Printing (PJD-3DP) is an Additive Manufacturing (AM) process that was developed by Objet Geometries, Ltd (Israel). In the process, layers of an acrylic-based photopolymer are selectively jetted onto a build-tray via inkjet printing (Figure 1). The jetted photopolymer droplets are immediately cured with ultraviolet lamps that are mounted onto the print carriage. The differentiating functionality of the PJD-3DP process (for the Connex machine line) is its ability to simultaneously jet multiple materials with different mechanical (and optical) properties. For example, by simultaneously jetting "TangoBlack" (an elastomeric material) and "VeroWhite" (a rigid polymer), a designer is able to manufacture products with functionally graded material properties. As such, PJD-3DP offers design freedom in specifying both the placement and the properties of materials on a point-by-point basis.

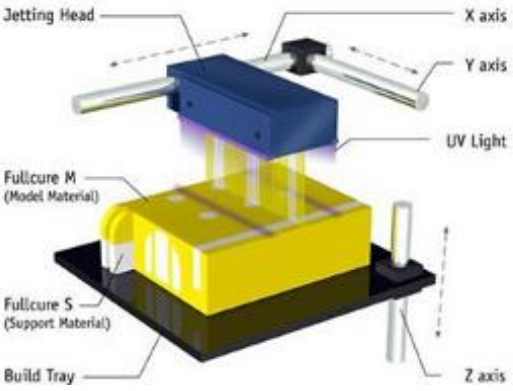

Figure 1. The PolyJet Direct 3DP Process [1]

While primarily used as a process for fabricating prototypes, the design freedoms offered by the process offer the opportunity to produce end-use products with unique, tailored geometries and materials. One example is Objet's marketing of FullCure 630 material, which is specifically formulated for the production of end-use custom-fit hearing aids. To be suitable for use as a manufacturing platform, the technology's structure/process/property relationships must be well established. However, as it is a relatively new AM process, research on this technology is still emerging.

1.1. AM Structure/Process/Property Relationships

Identifying structure/process/property relationships is critical for every manufacturing process; especially in AM where anisotropic properties can emerge due to material/energy patterning techniques, the build orientation of the part, and the interfaces between layers. Such research has been a key component of the advancement of all AM processes. For example, Agarwala and co-authors investigated how build strategies affect part porosity, and thus structural quality, in Freeform Filament Fabrication (FFF) [2]. Ahn and coauthors discovered that poor interlaying bonding in FFF contributed to significantly reduced tensile strength when parts were pulled perpendicular to the direction of layer construction [3]. Researchers have demonstrated that parts created by the Laser Sintering (LS) process are also anisotropic, with parts created as XY or XZ (part orientation and coordinate system used in ASTM F2921) were the strongest and parts oriented as ZX or ZY were the weakest [4, 5].

Existing research of the PJD-3DP process has primarily focused in characterizing the resultant parts. Pilipovic and coauthors note that their measured values for tensile strength are lower than that which is reported by Objet [6]. Udroui and Mihail experimentally determined that the "glossy surface" finishing option provided a higher quality surface roughness than the "matte surface" option [7]. Existing structure/process/property research is limited to Brajlih and coauthors' investigation of algorithms for scaling parts to improve process accuracy [8] and Kesy and Kotlinksi's exploration of the effects of part orientation on material properties [9]. While hardness was unaffected by orientation, both tensile strength and elongation at break were found to be lowest for parts created with XZ orientation.

Although structure/process/property relationships for PJD-3DP have not yet been fully defined, there perhaps is an opportunity to draw from established research in the stereolithography (SL) process, due to their common photopolymerization approach. Paul Jacob's extensive characterization of the SL process connects laser-based UV exposure of photopolymer resins to the cure depth of single vector scan to the mechanical properties of the finished part [10]. Specifically, elastic modulus and tensile strength increase (to a certain point) with increased exposure. This fundamental process characterization, which identifies the residual stresses caused by curing shrinkage [11, 12] and the "print-through" error caused by accumulated exposure across several layers, is linked to, and has driven the design of, SL laser scanning patterns [13]. SL process understanding has also provided a means of interpreting part anisotropy caused by varying layer thickness [14] and part orientation [15-17]. In [17] it was found that tensile samples oriented as XZ or YZ were statistically stronger than those printed flat on build tray as XY or YX due to differences in inter-layer bonding.

1.2. Research Scope

Although PJD-3DP and SL are functionally linked by their use of photopolymerization [18], the manner in which the UV irradiation is patterned is quite different. The vector scan-based approach of SL provides the ability to precisely pattern UV energy across the resin bath. The Objet process, however, selectively patterns resin while indiscriminately distributing UV energy via lamps mounted on the printing-block. Given that mechanical properties of photopolymer parts are so closely linked to the UV exposure, gaining an understanding of how PJD-3DP part properties relate to process parameters is paramount to ensuring its relevance and reliability as a manufacturing platform.

In this paper, the authors explore the process/property relationships of PJD-3DP via a design of experiments. Specifically, a full-factorial design is used to analyze the effects of three parameters on the specimens' tensile strength and tensile modulus: (i) the in-build plane part orientation (X-Y), (ii) the out-of-build plane part orientation (Z), (iii) and the distance between specimens. This work is guided by the research question, "*What controllable factors cause variability in the tensile strength and tensile modulus of VeroWhite parts manufactured through PolyJet Direct 3D Printing?*" The PolyJet process is detailed in Section 2. The experimental design is outlined in Section 3 and the experimental methods are presented in Section 4. Results and discussion are presented in Sections 5 and 6, respectively.

2. POLYJET DIRECT 3D PRINTING

As briefly described in Section 1, the PJD-3DP process features direct inkjet printing of photopolymer resin and subsequent curing by UV lamps. The Connex machine features eight print heads that can simultaneously print three materials: four heads are dedicated for jetting support material; the other four heads jet two distinct build materials. A small roller in the printing block flattens jetted droplets to provide an even surface for the deposition of subsequent layers. The process offers a relatively high resolution in the X-Y build plane (600 dpi printing resolution [19]) at small layer thicknesses (32 μm, or 16 μm in "High Quality" mode [19]). To provide scaffolding and stability to jetted droplets, printed parts are completely encased by the support material. The top-most surfaces are also typically coated in support material to provide an even surface finish (known as "matte finish"); however, the operator can choose to leave the top surface uncoated (known as "glossy finish"). Once the part has finished printing, the support material is removed from the part via a high-pressure water jet.

During printing, the print-block moves along the X-axis (Figure 2a) and deposits material in two back-and-forth translations (which constitutes a full "pass"). Jetting occurs only in the first forward translation; the remaining translations are solely to complete polymer curing. After completing a full pass, printing continues in the next printing "path" along the Y-axis of the build tray (Figure 2b). The extents of each printing path are defined by the width of the printheads. For example, the tensile specimens arranged on the build tray in Figure 2a each span three printing paths. The print-block offsets itself within each path between printing layers to fill in any voids that may have occurred due to clogged print nozzles.

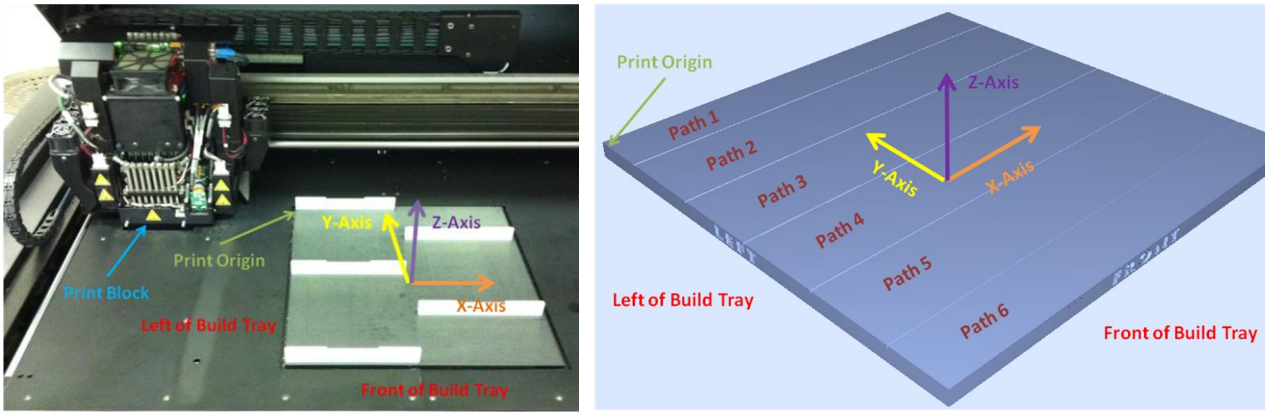

(a) (b)

Figure 2. Objet PJD-3DP Terminology

As translation between printing paths is a process bottleneck, the process's CAM interface (Objet Studio) automatically places parts in the build tray such that the longest dimensions are aligned along the X-axis, near the print origin. Additional "build rules" for orienting and placing parts within the build tray are presented in Table 1. These rules are derived as methods for minimizing total build time, minimizing support material consumption, and improving part surface quality. These rules are used for developing and selecting test parameters for experimental analysis, described in Section 3.

Table 1. Objet Build Rules [19]

Rule	Description	Effect	Rationale
X-Y-Z	• Place longest dimension along X-axis • Place intermediate dimension along Y-axis • Place smallest dimension in Z-axis	Reduced overall build time	• Reduce number of printing paths • Reduce total number of layers
Tall-Left	Place tallest part on the left of build tray	Reduced overall build time	Reduce translations needed by print-block to create part
Recess-Up	Orient indented surface features facing-up	Reduced total part cost	Reduce consumption of support material
Fine-Surface	Orient finely detailed features facing-up	Improved surface quality and lower cost	• Improved resolution along Z-axis • Reduce support material consumption

3. EXPERIMENTAL DESIGN AND METHODS

3.1. Parameter Selection

Given that mechanical properties of photopolymer parts are closely linked to UV exposure received (Section 1.1) and the manner in which the PJD-3DP process broadly patterns UV irradiation (Section 2), the authors hypothesize that a part's mechanical properties might be affected by build orientation and/or the spacing between parts across printing paths. While orientation in the X-Y and X-Z planes have been shown to cause variability in mechanical properties, the samples in that existing study were all printed simultaneously on the same tray, and thus did not account to variations in exposure levels during the print [9].

To identify process variability, the authors chose to employ a design of experiments for the PJD-3DP process. To properly analyze and select pertinent parameters, [19] and [20] were consulted based on their "Six Sigma" and quality control methodologies. An Ishikawa Diagram (aka Cause-and-Effect or Fishbone Diagram) was created based on the authors' knowledge of the PJD-3DP process (Section 2), and included potential factors that could produce deviation in the mechanical properties of VeroWhite material, as seen in Figure 3. Though this diagram does not guarantee nor reveal the true root cause, it was believed that through its graphical and organized structure, it would highlight the family where the root cause existed.

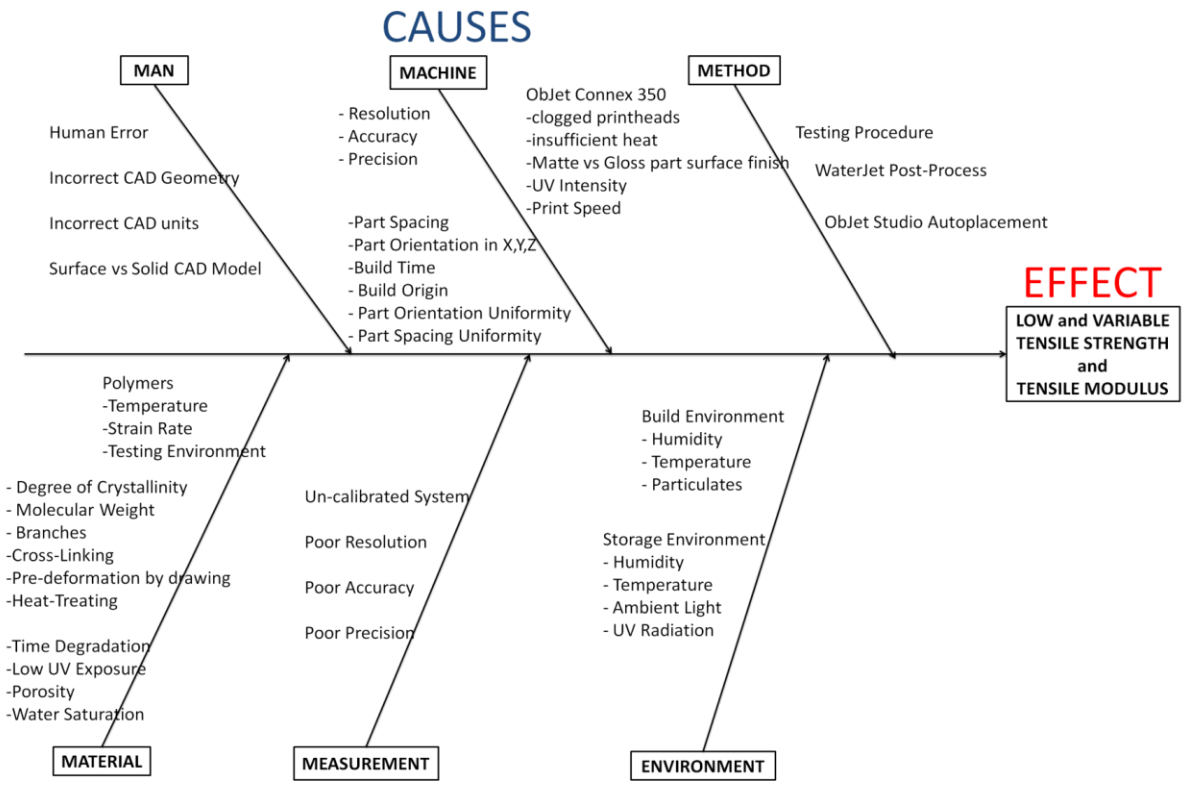

Figure 3. Ishikawa Diagram for PJD-3DP Process

Though many branches of the Ishikawa Diagram presented factors that could affect the material properties of the specimen, the "Machine" branch was further analyzed due to its uniqueness to PJD-3DP. Three parameters, believed to be the most pertinent and fundamental to creating PolyJet parts, were chosen for analysis in this study. A description for the selected parameters (X-Y Orientation, Z Orientation, and Part Spacing), and the rationale for their selection (i.e., hypothesized effect), is provided in Figure 4.

Parameter: X-Y Orientation

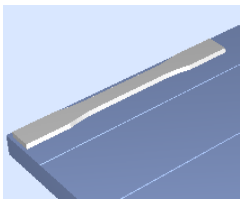

XY

Description: The in-plane build orientation of the part such that its length is parallel or perpendicular with respect to the front of the build tray.

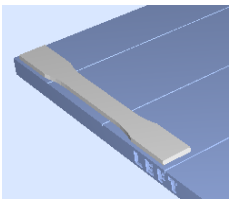

YX

Hypothesis: Orienting parts across print-head paths, may lead to lower mechanical properties due to banding from discretized jetting nozzles.

Parameter: Z-Orientation

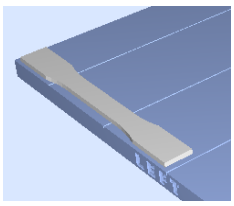

YX or XY (flat)

Description: The build direction orientation of the part such that the width, not the length, lays flat or angled with respect to the X-Y plane.

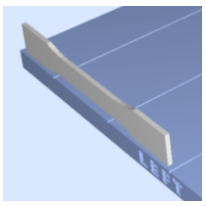

YZ or XZ (angled)

Hypothesis: An increase in the number of layers causes curing "print-through" and thus increased mechanical properties for parts with widths aligned in the Z plane (as noted for SL in [17]).

Parameter: Part Spacing

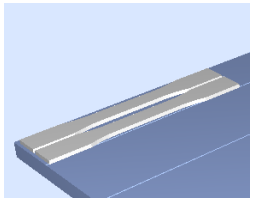

Tight Spacing

Description: The overall spacing between parts in X-Y plane of the build-tray.

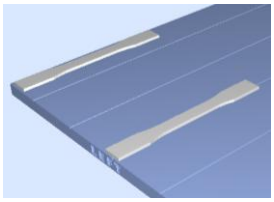

Far Spacing

Hypothesis: Smaller spacing may lead to increased mechanical properties due to potential UV over-cure effect.

Figure 4. Experimental Parameters

3.2. Design of Experiments

The goal of the experiments is to identify the variability in the mechanical properties (specifically, the tensile strength and modulus) of parts created using the VeroWhite resin. Objet specifies that Fullcure 830 Verowhite has a tensile Strength of 49.8 MPa and tensile modulus of 2495 MPa [22]. Following theory presented in [23], a three parameter and two-level full factorial design of experiments (DOE) was selected to analyze the effects of the three selected parameters. The two-level full factorial design was selected because the parameters could be easily varied at two discrete levels and statistically analyzed using only eight total experiments, making the DOE easy to regulate and execute due to low complexity.

Each parameter was varied at a "high" (+ 1) and "low" (-1) value and their effect on the tensile strength and modulus was measured. The full-factorial experiment is shown in Table 2. Each experiment was given a codified name to quickly identify the experiment and the levels of

the parameters. For example, “YXT” corresponds to an experiment with specimens oriented with lengths along the y-axis, widths along z-axis, and tight part spacing (Figure 5).

Table 2. Full Factorial Experiment

Parameters		**X-Y Orientation**		**Z-Orientation**		**Part Spacing**	
Levels		**YX (-1)**	**XY (+1)**	**YX or XY (-1)**	**YZ or XZ (+1)**	**Tight (-1)**	**Far (+1)**
Experiment Code Name	YXT	-1		-1		-1	
	YXF	-1		-1		1	
	YZT	-1		1		-1	
	YZF	-1		1		1	
	XYT	1		-1		-1	
	XYF	1		-1		1	
	XZT	1		1		-1	
	XZF	1		1		1	

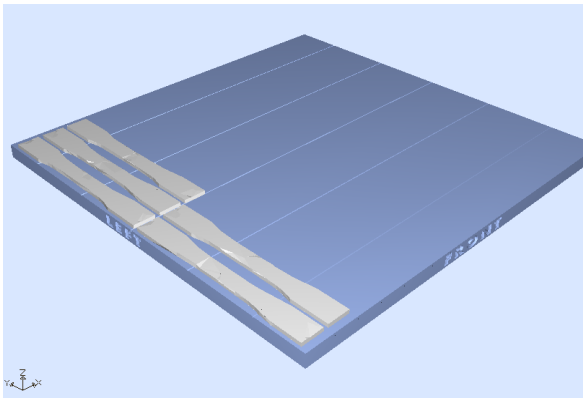

Figure 5. Build platform layout for “YXT” (specimens oriented in the y-axis, flat z-orientation, and tight part spacing) experiment.

3.3. Experimental Procedure

ASTM D638-10 was followed to measure specimens’ tensile strength and modulus. This standard has relevancy in engineering design and enables comparison across processes, including existing AM process analysis [17]. Figure 6 provides dimensional data for the selected "Type 1" tensile test specimen. Specimens’ thicknesses and widths were measured using a Marathon Electronic Digital Caliper (accuracy of 0.01 mm) to monitor any variable resolution and discrepancy. The specimens’ masses were measured on a digital scale (accuracy of 0.01g) were monitored to determine variation.

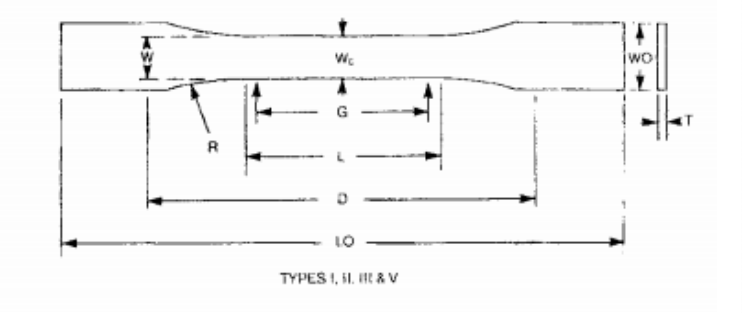

Dimensions (see drawings)	S 7 (0.28) or Type I
W—Width of narrow section[E,F]	13 (0.50)
L—Length of narrow section	57 (2.25)
WO—Width overall, min[G]	19 (0.75)
WO—Width overall, min[G]	...
LO—Length overall, min[H]	165 (6.5)
G—Gage length[I]	50 (2.00)
G—Gage length[I]	...
D—Distance between grips	115 (4.5)
R—Radius of fillet	76 (3.00)
RO—Outer radius (Type IV)	...

Figure 6. ASTM D638 Type 1 specimen dimensions

Each experiment (Table 2) was randomly chosen and printed using an Objet Connex 350. Parts were printed in "Digital Material Mode" with the "Matte" surface finish. Random selection prevents experimental bias and propagation of a consistent error [23]. Eight total build trays were printed in this study. Five specimens were printed per build tray, with each build tray corresponding to a specific experiment with uniform orientation among all printed specimen (no mixed orientations). Following the completed print job, specimens were cleaned using a high pressure waterjet. Upon drying, the specimens were conditioned at 72˚F in a closed opaque plastic container to prevent excess light exposure until ready for testing. Since [13] and [21] identify "time" as a possible degradation effect (due to oxygen levels and ambient light), the authors attempted to maintain a constant time between printing and testing for all experiments with a minimum conditioning period of 12 hrs. The authors also attempted to control the humidity of the conditioning specimens by storing the plastic container in metal cabinet located away from potential sources of moisture.

Tensile tests were conducted in the Virginia Tech Material's Testing Laboratory using an Instron 4468 Tensile Testing Machine in accordance to D638 standard. Using MTS Systems TestWorks for data acquisition with the Instron machine, tests were conducted at a stable environment of 72˚F and tested at a speed of testing of 50 mm/min (constant strain rate) until specimens ruptured. TestWorks was used to measure the applied force and strain of the specimen, which was then used to calculate the tensile strength and tensile modulus. The Tensile modulus was calculated using the Tangent Modulus method. Specimen elongation was measured with an axial clip-on extensometer (50% max strain). Test specimens were not tempered.

4. RESULTS

4.1. Experimental Data

The mean values for the metrics of each experiment are presented in Table 3. Standard deviation of tensile strength and modulus measurements are provided in parentheses.

Table 3. Mean Experimental Data

Experiment	Mass (g)	Thickness (mm)	Width (mm)	Tensile Strength (MPa)	Tensile Modulus (MPa)
YXT	10.1	3.23	13.4	32.3 (0.56)	1501 (32)
YXF	10.1	3.23	13.4	26.0 (1.06)	1577 (251)
YZT	10.5	3.59	13.0	31.2 (0.44)	1696 (240)
YZF	10.1	3.43	13.0	24.2 (2.62)	1176 (232)
XYT	10.0	3.25	13.4	35.3 (1.43)	1665 (73)
XYF	10.0	3.22	13.3	29.0 (1.50)	1719 (217)
XZT	10.8	3.66	13.0	37.8 (0.47)	1874 (89)
XZF	10.4	3.56	13.0	22.9 (0.43)	1284 (189)

Experiments fabricated with XZ and YZ orientations had thicknesses consistently in the 3.42-3.66 mm range compared to the D638 specification of 3.23 mm. A similar effect is also shown in that experiments fabricated with XY and YX orientations had widths consistently in the 13.3-13.4 mm range compared to the D638 specification of 13.0 mm. This suggests that Z-orientation can affect the accuracy of a part's thicknesses and widths.

The highest mean tensile strength was found in samples in the XZT experiment; the lowest occurred in the XZF experiment. The highest relative precision occurred in XZT with one standard deviation of 0.47 MPa (1.24 % its mean tensile strength) and the lowest occurred in YZF at 2.62 MPa (10.8 % of its mean). In comparison to Objet's quoted Verowhite tensile strength of 49.8 MPa [22], XZT had the lowest discrepancy at 12.0 MPa (24.1% of the quote) and XZF had the highest discrepancy at 26.9 MPa (54.0% of the quote). Figure 7 graphically summarizes the tensile strength data with one standard deviation and shows that experiments with the tight spacing consistently show higher mean tensile strength values than at far spacing.

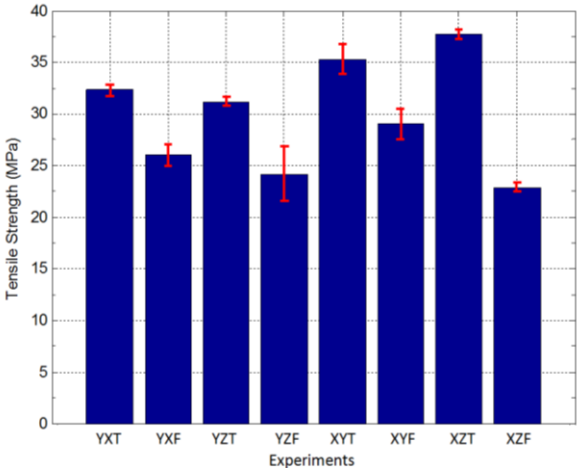

Figure 7. Mean tensile strength

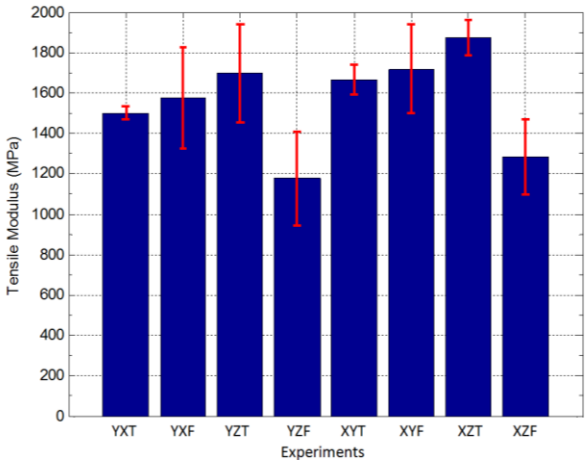

Figure 8. Mean tensile modulus

The highest tensile modulus occurred in the XZT experiment at a mean of 1874 MPa; the lowest occurred in YZF at a mean of 1176 MPa. The highest relative precision occurred in YXT with a sample standard deviation of 32 MPa (2.16 % of its mean tensile strength); the lowest occurred in YZF at 232 MPa (19.7 % of its mean). In comparison to Objet's quoted Verowhite Tensile Modulus of 2495 MPa [22], XZT again had the lowest discrepancy at 621 MPa (24.9% of the quote) and YZF had the highest discrepancy at 1319 MPa (52.9% of the quote). Figure 8 graphically summarizes the tensile modulus data. It is observed that all experiments with XZ or YZ orientation and tight part spacing showed higher mean tensile modulus values regardless of the orientation. A similar effect is shown in that the lowest mean tensile modulus occurred with specimen widths aligned with Z-axis with far part spacing regardless of In-Build Plane orientation.

4.2. Statistical Analysis

Using the experimental data, a factorial analysis was performed to determine the effects of a parameter and its interactions on tensile strength and modulus (Tables 4 and 5).

Table 5. Tensile Strength Factorial Analysis

	MAIN EFFECTS						2nd ORDER INTERACTIONS						3rd ORDER	
Parameter	A (X-Y Orientation)		B (Z-Orientation)		C (Part Spacing)		A*B		A*C		B*C		A*B*C	
Parameter Level	YX (-1)	XY (+1)	YX or XY (-1)	YZ or XZ (+1)	Tight (-1)	Far (+1)	-1	1	-1	1	-1	1	-1	1
Average Response	28.4	31.2	30.6	29.0	34.1	25.5	29.9	29.7	30.8	28.8	31.0	28.7	30.8	28.8
Effect	2.9		-1.7		-8.6		-0.2		-2.0		-2.3		-2.0	

Table 6. Tensile Modulus Factorial Analysis

	MAIN EFFECTS						2nd ORDER INTERACTIONS						3rd ORDER	
Parameter	A (X-Y Orientation)		B (Z-Orientation)		C (Part Spacing)		A*B		A*C		B*C		A*B*C	
Parameter Level	YX (-1)	XY (+1)	YX or XY (-1)	YZ or XZ (+1)	Tight (-1)	Far (+1)	-1	1	-1	1	-1	1	-1	1
Average Response	1488	1636	1616	1508	1684	1439	1564	1559	1573	1550	1717	1407	1568	1556
Effect	148		-108		--245		-5		-23		-310		-12	

The factorial analysis was then used to produce normal probability plots, Figures 9 and 10. These plots are a statistical technique for graphically estimating which main and interaction effects have statistical significance. Assuming the validity of the Central Limit Theorem [23], measured effects from a consistent process will appear to be from a normal distribution therefore, a potentially statistically significant effect would be an outlier.

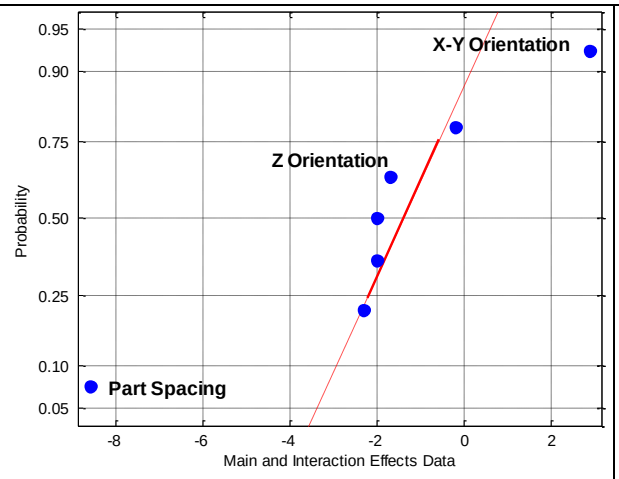

Figure 9. Tensile strength normal probability plot

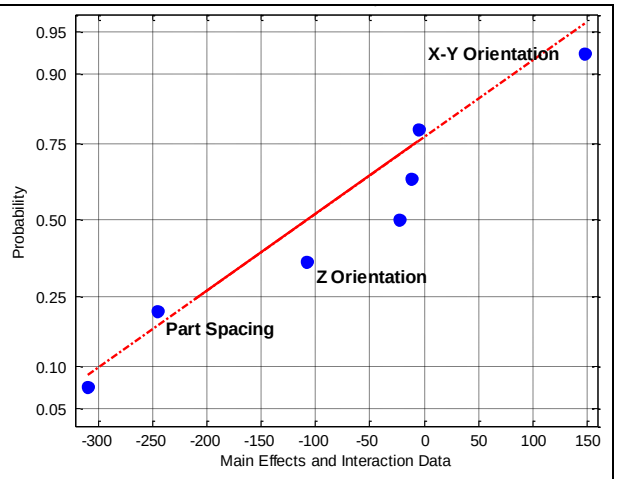

Figure 10. Tensile modulus normal probability plot

For the tensile strength, the factorial analysis revealed that the largest absolute effect was the part spacing, which could vary the response by 8.6 MPa. Figure 9 shows that a majority of the effects and interactions appear to be from the normal distribution but, the Part Spacing may be the only statistically significant effect on the Tensile Strength. For the tensile modulus, the interaction between the Z-orientation and the part spacing produced the largest absolute effect at 310 MPa. The normal probability plot shows that all effects and interactions appeared to be from the normal distribution suggesting that none of them may have statistically significant effects on

the tensile modulus. While the part spacing was the largest absolute main effect for both responses, the Z-orientation was the smallest absolute main effect for both.

4.3. Analysis of Variance (ANOVA)

Given that the Z-orientation parameter had the smallest absolute main effect, and appeared to be from the normal distribution for both the tensile strength and modulus (Figures 9 and 10), it was assumed to be statistically insignificant. This assumption permits the treatment of the performed three parameter and two level full-factorial design as a pseudo-replicated two parameter and two level full-factorial design (i.e., YXT to YZT and YZF to YXF were considered replicated experiments) [23]. By using this pseudo-replication, Analysis of Variance (ANOVA) could be performed on the two remaining effects (X-Y orientation and Part Spacing) and their interactions. ANOVA is a statistical technique in which the sum of squares and error terms are compared against an F-ratio statistic along with p-values to determine the statistical significance of the parameters.

Using SAS JMP, a statistical analysis software, experimental data was used in a "Fit Model" to define a two-level and two parameter full factorial design to perform an ANOVA. The DOE was modeled using a "Standard Least Squares" behavior. Each effect and interaction had its F-ratio calculated and compared against the critical F-ratio calculated at an alpha-value of 0.05. The ANOVA for Tensile Strength and Modulus is shown in Figure 11 and 12 below.

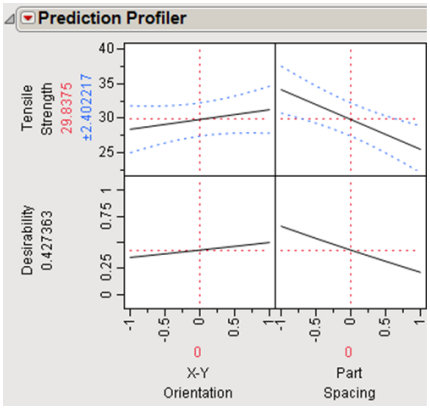

Parameter Estimates

Term	Estimate	Std Error	t Ratio	Prob>|t|
Intercept	29.8375	0.865213	34.49	<.0001*
X-Y Orientation	1.4125	0.865213	1.63	0.1779
Part Spacing	-4.3125	0.865213	-4.98	0.0076*
X-Y Orientation*Part Spacing	-0.9875	0.865213	-1.14	0.3174

Effect Tests

Source	Nparm	DF	Sum of Squares	F Ratio	Prob > F
X-Y Orientation	1	1	15.96125	2.6652	0.1779
Part Spacing	1	1	148.78125	24.8435	0.0076*
X-Y Orientation*Part Spacing	1	1	7.80125	1.3027	0.3174

Figure 11. Tensile Strength ANOVA

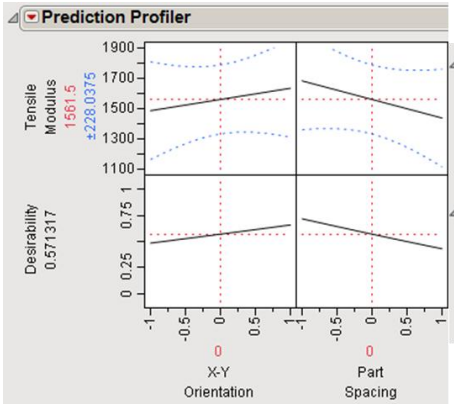

Parameter Estimates

Term	Estimate	Std Error	t Ratio	Prob>|t|
Intercept	1561.5	82.1329	19.01	<.0001*
X-Y Orientation	74	82.1329	0.90	0.4185
Part Spacing	-122.5	82.1329	-1.49	0.2101
X-Y Orientation*Part Spacing	-11.5	82.1329	-0.14	0.8954

Effect Tests

Source	Nparm	DF	Sum of Squares	F Ratio	Prob > F
X-Y Orientation	1	1	43808.00	0.8118	0.4185
Part Spacing	1	1	120050.00	2.2245	0.2101
X-Y Orientation*Part Spacing	1	1	1058.00	0.0196	0.8954

Figure 12. Tensile Strength ANOVA

4.4. Interpreting ANOVA

The ANOVA analysis of tensile strength provided an R-squared value of 0.88 and a RMSE of 2.45%, indicating an adequate correlation between the experimental data and the model suggesting the model is sufficient for prediction, due to minimal residuals and random noise. The factorial analysis in Figure 11's "Parameter Estimates" shows that the part spacing's was the largest absolute effect at 8.63 MPa, (which is approximately equal to the value from earlier analysis (Table 5). Its F-ratio of 24.8 is the only value that exceeds the critical F-ratio of 9.60 and its 0.0076 p-value is nearly an order of magnitude smaller than the 0.05 alpha value. Based on these two criteria, part spacing is the only statistically significant effect on the tensile strength.

The tensile modulus ANOVA has an R-squared value of 0.43 but a RMSE of 232% which indicates that large residuals and a very large amount of noise exists in the data, suggesting that the model is not very adequate to predict the data. Figure 12's "Parameter Estimates" show that the part spacing had the largest absolute effect at 122 MPa, which is not approximately equal to the value found in earlier factorial analysis (Table 6). This discrepancy is due to the interaction effect between the part spacing and Z-orientation, which is confounded with the part spacing in this ANOVA. While part spacing's F-ratio of 2.22 does exceed the critical F-ratio of 1.02, further analysis reveals that its 0.210 p-value is greater than the alpha value. Despite having a large F-ratio, part spacing and other effects are not statistically significant due to p-values greater than the alpha value, indicating a higher risk of Type I error.

5. DISCUSSION

5.1. Analysis of Results

Synthesizing the experimental data presented in Section 4, the following results are identified:

- Part dimensions aligned in the X-Y plane were fabricated 200-400 μm larger than designed (Table 3). This suggests that Z-orientation can affect the accuracy of a part's thicknesses and widths. This result is not surprising given that the Z-resolution of the PJD-3DP process (32-60 mm layer thickness) is better than the X-Y printing resolution (600 dpi). This is result is unique to the PJD-3DP process as most AM processes have poor dimensional accuracy for features aligned along the Z-axis due to the discretized nature of the layer-by-layer approach.
- XY and YX parts did not show any statistically significant effects on material performance. The authors' hypothesis that YX oriented parts would be weaker due to jetting from discretized nozzles was found to be incorrect. XY and XZ parts were, on average, stronger; however, the results were not statistically significant.
- Parts oriented in the Z-plane did not show any statistically significant improvements in material performance. The authors' hypothesis that parts with XZ and YZ orientation would be stronger due to an increase in the number of layers (and thus lead to increased curing due to "print-through", as noted for SL in [17]) was incorrect. Specimens with widths along the Z-axis were, on average, stronger; however the results were not statistically significant.

- Part spacing in the X-Y plane showed statistically significant effects on material performance. As hypothesized by the authors, parts printed closer together in the X-Y plane were stronger than parts printed further apart. This increase in material properties is hypothesized to be related to the manner in which the PJD-3DP indiscriminately patterns UV light during processing. Thus, when printing multiple parts that span multiple print paths, UV irradiation from the printing-block can over-cure parts in paths adjacent to the current printing path.

5.2. Sources of Experimental Error

The weakness of DOE is that there are no immediately replicated results to verify and validate the completed DOE. While ANOVA helps eliminate unnecessary variables, its success is based on the quality and precision of the collected data, in which replication would provide the best insurance for determining the consistency of the data. Full-factorial DOE's provide the highest quality and resolution in an experiment but considering each combination of parameter level can be time-consuming and lead to excessive use of resources. While a pseudo-replication can enable ANOVA for two parameters (Section 4.4), this assumption removes a parameter which provides less precision and insight as to how the original three parameters truly interacted together. For example, while factorial analysis did not suggest that Part Spacing and Z-orientation had statistical significance, they had a practical significance in that their interaction was the largest absolute effect on the tensile modulus.

In addition to error in statistical techniques, the lifetime of parts (i.e., time between print start and tensile test) was not consistent between experiments. This is important because time is suspected to be a potential cause of polymer aging and degradation [21]. In addition, differences of relative humidity between experiments and testing were not explicitly controlled; humidity can affect mechanical properties since polymers are hygroscopic and could have softened surfaces due to ambient moisture [24]. Finally, it is noted that a potential source of differentiation between the measured values with that specified by Objet could be due to their use of ASTM D638-03 and D638-04 [25], which might have different test specimens and conditions for testing and/or the authors' use of "Digital Material" mode instead of "High Quality" mode during sample fabrication.

6. CLOSURE

The purpose of this study was to analyze variability in the mechanical properties of parts created by the PolyJet Direct 3D Printing process due to changes in process parameters. The authors employed a design of experiments to identify changes in part tensile strength and tensile modulus due to changes in X-Y orientation, Z-orientation, and part spacing in the X-Y plane. ANOVA revealed that part spacing had a statistically significant effect on mechanical properties; specifically, parts printed closer together were stronger than those printed farther apart.

Future studies will further investigate the effect of part spacing on mechanical properties. The authors will explore the hypothesis that the PJD-3DP process is over-curing parts across multiple print paths. An AM process wherein part quality is affected by its layout on the build platform could have significant impact on a designer's ability to predict part performance – in

effect, part properties would be inconsistent across various build platforms (due to part count and/or size).

7. ACKNOWLEDGEMENTS

The authors acknowledge Daniel Dressner (Virginia Tech ME, ’12) for his preliminary investigation in effects of build orientation on mechanical properties in the PJD-3DP process. The authors also acknowledge Mac McCord of Virginia Tech Material's Testing Laboratory for his assistance with tensile testing.

8. REFERENCES

[1] "Objet Polyjet Process." *Objet Geometries Ltd.* Www.Objet.com, n.d. Web. <http://www.objet.com/products/polyjet_technology/>.

[2] Agarwala, M. K., V. R. Jamalabad, N. A. Langrana, A. Safari, P. J. Whalen and S. C. Danforth, 1996, "Structural Quality of Parts Processed by Fused Deposition," *Rapid Prototyping* Journal, Vol. 2, No. 4, p. 4-19.

[3] Ahn, S-H, M. Montero, D. Odell, S. Roundy and P. K. Wright, 2002, “Anisotropic material properties of fused deposition modeling ABS,” *Rapid Prototyping Journal*, Vol. 8, No. 4, p. 248 – 257.

[4] Gibson, I. and D. Shi, “Material properties and fabrication parameters in selective laser sintering process,” *Rapid Prototyping Journal*, Vol. 3, No. 4, p. 129–136.

[5] Ajoku, U., N. Salesh, R. J. M. Hague, P. Erasenthiran, 2006, “Investing mechanical anisotropy and end-of-vector effect in laser-sintered nylon parts,” *Journal of Engineering Manufacture*, Vol. 220, No. 7, p. 1077–1086.

[6] Pilipovic, A., P. Raos and M. Sercer, 2009, “Experimental analysis of properties of materials for rapid prototyping,” *International Journal of Advanced Manufacturing Technology*, Vol. 40, p. 105-115.

[7] Udroiu, R. and L. A. Mihail, 2009, “Experimental determination of surface roughness of parts obtained by rapid prototyping,” *CSECS'09 Proceedings of the 8th WSEAS International Conference on Circuits, Systems, Electronics, Control & Signal Processing*, p. 283-286

[8] Brajlih, T., I. Drstvensek, M. Kovacic, J. Balic, 2006, “Optimizing scale factors of the PolyJet rapid prototyping procedure by genetic programming,” *Journal of Achievements in Materials and Manufacturing Engineering*, Vol. 16, No. 1-2, p. 101-106.

[9] Kesy, A. and J. Kotlinksi, 2010, “Mechanical properties of parts produced by using polymer jetting technology,” *Archives of Civil and Mechanical Engineering*, Vol. X, No. 3, p. 37-50.

[10] P. F. Jacobs, 1996, *Stereolithography and other RP&M Technologies: from Rapid Prototyping to Rapid Tooling*, ASME Press, New York, NY.

[11] Lu, L., J. Y. H. Fuh, A. Y. C. Nee, E. T. Kang, T. Miyazawa, and C. M. Cheah, 1995, “Origin of shrinkage, distortion, and fracture of photopolymerized material,” *Materials Research Bulletin*, Vol. 30, No. 12, p. 1561-1569.

[12] Karalekas, D. and D. Rapti, 2002, “Investigation of the processing dependence of SL solidification residual stresses,” *Rapid Prototyping Journal*, Vol. 8, No. 4, p. 243-247.
[13] Gibson, I., D. W. Rosen, and B. Stucker, 2010, *Additive Manufacturing Technologies: Rapid Prototyping to Direct Digital Manufacturing*, Springer, New York, NY.
[14] Chockalingam, K. and N. Jawar, 2006, “Influence of layer thickness on mechanical properties in stereolithography,” *Rapid Prototyping Journal*, Vol. 12, No. 2, p. 106-113.
[15] Hague, R., S. Mansour, N. Saleh, and R. Harris, 2004, “Materials analysis of stereolithography resins for use in rapid manufacturing,” *Journal of Materials Science,* Vol. 39, p. 2457-2464.
[16] Dulieu-Barton, J. M. and M. C. Fulton, 2000, “Mechanical properties of a typical stereolithography resin,” *Strain*, Vol. 36, No. 2, p. 81-87.
[17] Quintana, R., J-W Choi, K. Puebla, and R. Wicker, 2009, “Effects of build orientation on tensile strength for stereolithography-manufactured ASTM D-638 type I specimens,” *International Journal of Advanced Manufacturing Technology*, Vol. 46, No. 1-4, p. 201-215.
[18] Williams, C. B., F. Mistree, and D. W. Rosen, 2011, “A functional classification framework for the conceptual design of additive manufacturing technologies,” *Journal of Mechanical Design*, Vol. 133, p. 121002-1 – 121002-11.
[19] "Connex Family: The Polyjet Matrix System Operator Training Guide," Objet Geometries Ltd., 2009. Print.
[20] Bhote, Keki R., and Adi K. . Bhote. *World Class Quality*. New York: Amacom, 2000. Print.
[21] Gibson, I., G. Goenka, R. Narasimhan, and N. Bhat, 2010, “Design Rules for Additive Manufacture,” *International Solid Free Form Fabrication Symposium*, Austin, TX.
[22] "Fullcure Materials." *www.objet.com*. Objet Geometries Ltd., Web. 5 Jan. 2011. <http://www.objet.com/portals/0/docs2/FullCure_Letter_low.pdf>.
[23] Vining, G. G. and S. M. Kowalski, 2011, *Statistical Methods for Engineers*, Cengage Learning, Boston, MA.
[24] Callister, William D. *Materials Science and Engineering: An Introduction*. Hoboken, NJ: John Wiley & Sons, 2006. Print.
[25] “Digitial Material Data Sheets," Objet Geometries Ltd., Web. 2012. <http://www.objet.com/Portals/0/docs2/Digital%20Materials_Datasheet_A4.pdf>